

Luminescence properties of Eu^{2+} activated $\text{Ba}_2\text{Si}_5\text{N}_8$ red phosphors with various Eu^{2+} contents

Jun-Myung Song^a, Joo-Seok Park^{a,*}, Sahn Nahm^b

^aEnergy Storage Center, Korea Institute of Energy Research, Jang-dong, Yuseong-gu, Daejeon 305-343, Korea

^bDepartment of Materials Science and Engineering, Korea University, 1-5 Ka Anam-dong, Seongbuk-gu, Seoul 136-701, Korea

Received 25 June 2012; received in revised form 7 September 2012; accepted 15 September 2012

Available online 9 October 2012

Abstract

This study was carried out to characterize the crystal structure and luminescence properties of Eu^{2+} doped red-emitting $\text{Ba}_2\text{Si}_5\text{N}_8$ phosphor. In this research, $\text{Ba}_2\text{Si}_5\text{N}_8$ phosphors with various Eu compositions were prepared by normal pressure sintering (NPS). Ba_3N_2 , Si_3N_4 and Eu_2O_3 were sintered at a high temperature in a mixture of N_2 and H_2 . The crystal structure was analyzed by X-ray diffraction (XRD), and the photoluminescence (PL) properties of the Eu^{2+} -activated $\text{Ba}_2\text{Si}_5\text{N}_8$ phosphors were evaluated as a function of the Eu^{2+} activator concentration. The red-emitting $\text{Ba}_2\text{Si}_5\text{N}_8$ phosphors showed a broad excitation band range as well as high quantum output.

Crown Copyright © 2012 Published by Elsevier Ltd and Techna Group S.r.l. All rights reserved.

Keywords: $\text{Ba}_2\text{Si}_5\text{N}_8$; Nitride phosphor; Red phosphor; Normal pressure sintering

1. Introduction

Luminescent material, also called a phosphor, is a solid which converts certain type of energy into electromagnetic radiation over and above thermal radiation. Even though a number of new phosphors have been synthesized and investigated [1,2], red phosphors, such as oxides and sulfide, are not desirable, as they possess either low luminescence efficiency or bad stability. In order to achieve for high color rendering index and sufficient color reproducibility for general lighting and liquid crystal display backlight, it is desired to develop highly-efficient red phosphor with sufficient chemical durability and ideal luminescent properties. Eu^{2+} doped $\text{M}_2\text{Si}_5\text{N}_8$ ($M = \text{Ca}, \text{Sr}, \text{Ba}$), an efficient red-emitting phosphor, has been developed only recently [3–5]. $\text{M}_2\text{Si}_5\text{N}_8$ has many advantages, including high quantum output, high stability, and excellent temperature characteristics, and it seems to be particularly promising for applications in which saturated red emission is required. Although Mn^{2+} also can be used as an activator of $\text{M}_2\text{Si}_5\text{N}_8$ ($M = \text{Ca},$

Sr, Ba) [6], Ce^{3+} and Eu^{2+} show long-wavelength emission in $\text{M}_2\text{Si}_5\text{N}_8$ host lattice ($M = \text{Ca}, \text{Sr}, \text{Ba}$), due to the high covalency and large crystal field effect of nitrogen anion. Especially, Eu^{2+} is the most well-known and widely applied rare earth ion. The phosphor doped with Eu^{2+} ($4f^7$) emits longer-wavelength light owing to the $4f \rightarrow 5d$ transition. As d electrons participate in the chemical bonding, the d-f emission spectra consist of broad bands. Furthermore, the d-f optical transitions are allowed and are consequently very fast [7–10]. Nevertheless, a number of problems related to this phosphor need to be addressed, for example, in some cases, it is quite difficult to stabilize Eu^{2+} [11] because of its lower stability compared with Eu^{3+} . In most case, the emission of phosphor doped with Eu^{3+} ($4f^7$) is due to optical transitions with the f-manifold. The f-electrons are well shield from the chemical environment and therefore have almost retained their atomic character. It is attributed to the higher electronegativity and nephelauxetic effect of the N^{3-} ion, which effectively lowers the gravity center of the 4b orbital of Eu^{2+} ions.

RE nitride phosphor have been synthesized by several methods [12–14]. Up to now, commercial red-emitting phosphors have been synthesized mainly by gas pressure sintering (GPS). However the GPS method is disadvantageous in

*Corresponding author. Tel.: +82 42 860 3443; fax: +82 42 860 3769.
E-mail address: jspark@kier.re.kr (J.-S. Park).

terms of the high manufacturing cost involved. Eu^{2+} doped $\text{M}_2\text{Si}_5\text{N}_8$ ($M=\text{Ca}, \text{Sr}, \text{Ba}$) is difficult to improve the luminescence properties, the sintering conditions such as temperature, holding time, and gas partial pressure should be optimized. Therefore, a new fabrication method called normal pressure sintering(NPS) has been adopted; this method affords phosphors that show strong photoluminescence(PL).

In this study, $\text{Ba}_2\text{Si}_5\text{N}_8$ was prepared using the NPS method. The effect of Eu^{2+} concentration on the luminescence properties was investigated and explained; further, the luminescence characteristics were evaluated at different temperatures.

2. Experimental

2.1. Nitride mixture preparation

Ba_3N_2 (High Purity Chemicals), Si_3N_4 (H.C. Stock), and Eu_2O_3 (Metal China) were weighed to prepare the $\text{Ba}_2\text{Si}_5\text{N}_8$ mixture. The nitrides and europium oxide were mixed in the ratio $\text{Ba}:\text{Eu}:\text{Si}=2-x:x:5$. The molar concentration of Eu was varied from 0.1 mol to 0.2 mol in increments of 0.025 mol. The raw materials were mixed using an agate mortar. All these processes were carried out in a purified nitrogen glove box. To prevent oxidation, the oxygen and moisture concentrations were maintained below 0.1 ppm.

2.2. Sintering

The mixed powders were transferred to a Mo crucible, which was then loaded into the NPS apparatus equipped with a tube furnace. After evacuation, the tube was sintered at a high temperature 1620–1700 °C for 2 h under 70% N_2 + 30% H_2 Flow.

2.3. Analysis and evaluation

The sintered phosphor was ground using an agate mortar. The crystal structure of the phosphors was obtained using an X-ray diffractometer (RIGAKU, Dmax-2500 pc, JAPAN) with $\text{CuK}\alpha$ ($=1.5408 \text{ \AA}$) radiation, at 40 kV, and 30 mA. The morphology of the phosphor particles were confirmed by scanning electron microscopy(SEM; HITACH S-4800, Japan). The mean particle size and standard deviation were determined by the PSA soft-ware equipped with SEM. The diffuse reflection, emission and excitation spectra of the samples were measured at room temperature using a Perkin-Elmer LS 55 spectrophotometer equipped with a Xenon lamp as an excitation source(operating voltage: 681 V; scan speed: 10 nm/min; in slit: 10 nm; out slit: 10 nm). The temperature dependence of PL was measured using a multichannel analyzer equipped with temperature-controlled sample holders. Quantum efficiencies(QE) were measured by PL Measurements(PSI Spectrum Analyzer DARSA-5200). This measurement consists of a xenon arc lamp, a monochromator, a BaSO_4 -coated integrating sphere, a multichannel detector and a personal computer. A monochromatic light source was used as the excitation light source, which comprised a xenon lamp with a lamp rating 150 W. The excitation light was introduced into the integrating sphere by optical fiber. The integrating sphere contains baffle between the sample and detection exit positions to prevent direct detection of the excitation light and emission from the sample and the baffles are also coated with light reflective material barium sulfate.

3. Results and discussion.

3.1. XRD analysis

Fig. 1 shows the X-ray diffraction(XRD) patterns of $\text{Ba}_2\text{Si}_5\text{N}_8:\text{Eu}^{2+}$ phosphors with different Eu^{2+} concentrations. All the samples appeared to crystallize in an

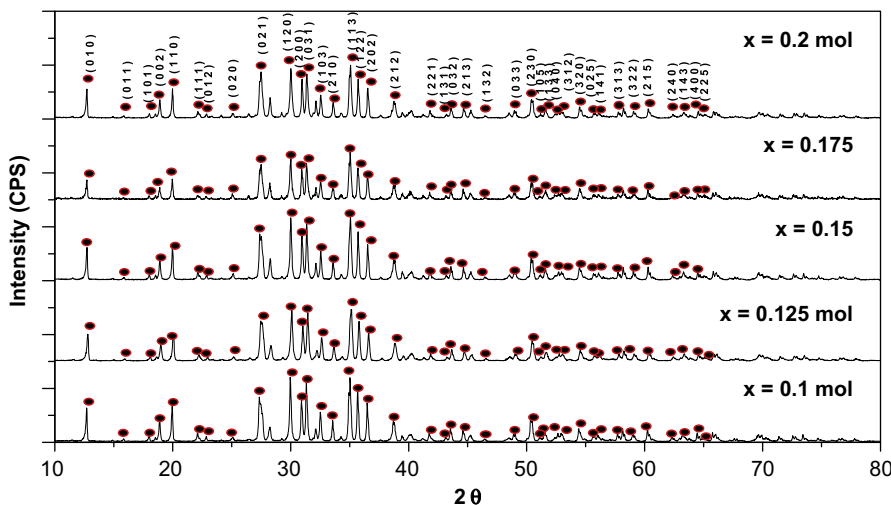


Fig. 1. XRD patterns of $\text{Ba}_2\text{Si}_5\text{N}_8$ phosphors with different Eu^{2+} concentrations. The molar concentration of Eu was varied from 0.1 mol to 0.2 mol at intervals of 0.025 mol.

orthorhombic unit cell (JCPDS 97-040-1501). There was no observable difference between these diffraction patterns. Almost all the diffraction peaks well matched with the standard JCPDS card of $\text{Ba}_2\text{Si}_5\text{N}_8$. However, the observed patterns differed slightly from the reported $\text{Ba}_2\text{Si}_5\text{N}_8$ (JCPDS 97-040-1501) pattern at $2\theta=29^\circ\sim 30^\circ$ and $2\theta=39^\circ\sim 41^\circ$, probably because of some unknown secondary phase formed by oxidation during the sintering process and the impurities in the raw materials. The structure parameters are listed in Table 1. The cell volume decreased by about 2% upon substitution with Eu^{2+} . In spite of the presence of the secondary phase, the unit cell volume of $\text{Ba}_2\text{Si}_5\text{N}_8:\text{Eu}^{2+}$ decreased almost linearly with an increase in x , because of the replacement of Ba^{2+} with the smaller Eu^{2+} ion [15], in agreement with Vegard's law.

3.2. SEM analysis of phosphors

Fig. 2 shows the SEM images of the $\text{Ba}_2\text{Si}_5\text{N}_8$ powders. The microstructures of the phosphors consisted of irregular grains with heavy agglomeration. Some parts were broken up during

grinding in agate. The results showed that the $\text{Ba}_2\text{Si}_5\text{N}_8$ phosphors have good crystallinity but consist of irregular primary spherical crystals. The particle size is an important parameter for the phosphor converted white light emitting diode application. In the wet method using laser beams the solid particle is normally dispersed in water or in organic solutions, therefore sometimes the fine small particles agglomerate together to form larger particles likely clusters. So the nozzle of the analyzer was frequently clogged and induced to be taken out of order. In the other hand the dry method using scanning electron microscope the particle size was determined by the automated particle analyzer equipped with SEM. So it is so much convenient to prepare and to easily determine its size and distribution. Furthermore we are able to determine 1.12 ± 0.5 , 0.68 ± 0.2 , 1.42 ± 0.7 , 1.12 ± 0.5 , and $1.52 \pm 0.4 \mu\text{m}$ directly magnified to $2 \times 10^4 \sim 5$ times their actual size.

3.3. Photoluminescence of $\text{Ba}_2\text{Si}_5\text{N}_8$

Fig. 3 presents the PL excitation and emission spectra of $\text{Ba}_2\text{Si}_5\text{N}_8:\text{Eu}^{2+}$ at room temperature. The excitation band

Table 1
Lattice parameters and unit-cell volumes of $\text{Ba}_2\text{Si}_5\text{N}_8$ phosphors with different Eu^{2+} concentrations (x mol).

x	0.1 mol	0.125 mol	0.15 mol	0.175 mol	0.2 mol
$a(\text{\AA})$	5.7794	5.7712	5.7712	5.7760	5.7711
$b(\text{\AA})$	6.39486	6.9119	6.9041	6.9433	6.9180
$c(\text{\AA})$	9.3667	9.4089	9.3935	9.2860	9.2519
$V(\text{\AA}^3)$	376.1548	375.3206	374.3418	372.4426	369.3772

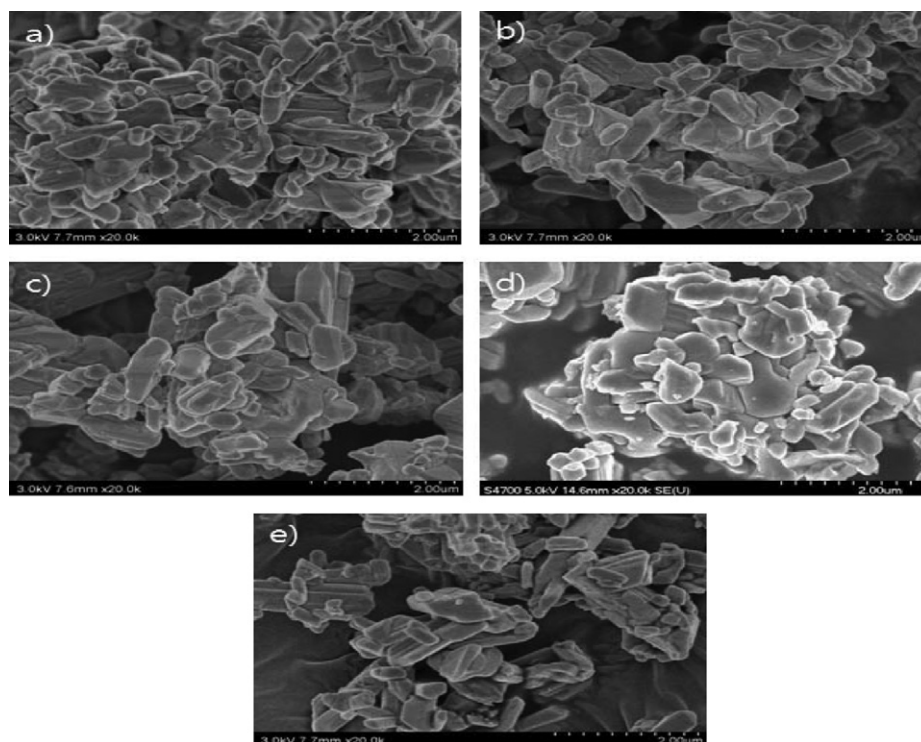


Fig. 2. SEM images of $\text{Ba}_2\text{Si}_5\text{N}_8$ powders with different concentrations of Eu^{2+} : a) 0.1 mol, b) 0.125 mol, c) 0.15 mol, d) 0.175 mol, and e) 0.2 mol.

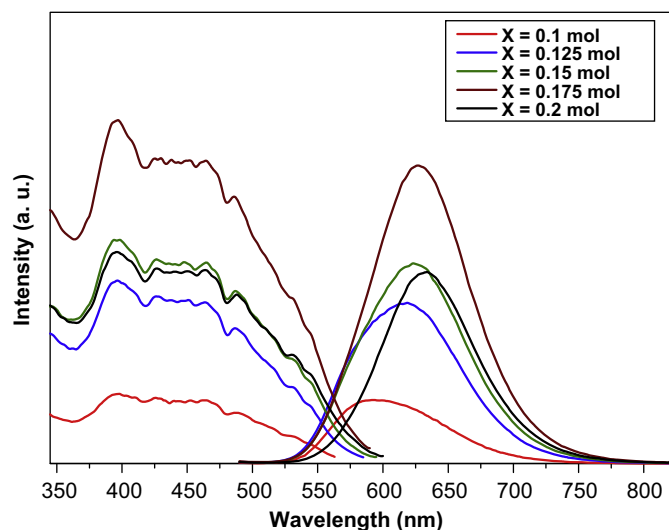


Fig. 3. Excitation and emission spectra of $\text{Ba}_2\text{Si}_5\text{N}_8$ phosphors with different Eu^{2+} concentrations.

below 395 nm could be ascribed to the transition between the valence and conduction bands of the host. The excitation energy was transferred from the host to the activator Eu^{2+} resulting in red-light emission. All the $\text{Ba}_2\text{Si}_5\text{N}_8:\text{Eu}^{2+}$ phosphors exhibited a red emission corresponding to the central position of the emission band from the $f \rightarrow d$ transition of Eu^{2+} . The $\text{Ba}_2\text{Si}_5\text{N}_8:\text{Eu}^{2+}$ phosphors showed a broad symmetric band in the wavelength range 500–700 nm, with the peak center at 593, 615, 623, 627, and 633 nm.

This broad luminescence band of Eu^{2+} was due to the $4f^6 5d^1 \rightarrow 4f^7$ transition, which is an allowed electric dipole transition. It is attributed to the higher electronegativity and nephelauxetic effect of the N^{3-} ion, which effectively lowers the gravity center of the 4d orbital of Eu^{2+} ions. The effect of the doped- Eu^{2+} concentration on the emission of the $\text{Ba}_2\text{Si}_5\text{N}_8:\text{Eu}^{2+}$ phosphors was also investigated. When the Eu^{2+} concentration was increased from 0.1 mol to 0.2 mol in steps of 0.025 mol, the emission band showed a redshift from 593 nm to 633 nm. As more Eu^{2+} ions replaced the Ba^{2+} ions, the strength of the crystal field increased, which in turn resulted in the redshift. The redshifted band rises at higher x -values. [16] The PL intensity increased with the Eu^{2+} concentration, reached the maximum value $x = 0.175$ mol, and then decreased because of concentration quenching. This result indicated that the optimum concentration of the Eu^{2+} for $\text{Ba}_2\text{Si}_5\text{N}_8:\text{Eu}^{2+}$ phosphors synthesized by NPS is 0.175 mol. The decrease in the emission intensity was because of the non-radiative energy transfer between the Eu^{2+} ions, which is dependent on the interionic distance according to Dexter's theory [17]. As the concentration of the Eu^{2+} ions increased, the distance between the Eu^{2+} ions decreased, causing non-radiative energy transfer between the Eu^{2+} ions to become the preferred mode of energy transfer. This is a suitable explanation for the concentration quenching, which is attributed to energy migration.

3.4. Luminescence characteristics at different temperatures

In order to characterize the luminescence properties of $\text{Ba}_2\text{Si}_5\text{N}_8:\text{Eu}^{2+}$, in further detail, the thermal quenching effect was investigated. In general, the temperature dependence of phosphors used in phosphor-conversion white LEDs is important because it has considerable influence on the light output and color rendering index. Since junction temperature increase with rising current, the degradation of luminescence efficiency and shift of chromaticity are the key issue for the white LEDs especially for the high-power ones. The luminescence spectra were recorded at different temperatures (Fig. 4). A gradual reduction in the luminescence intensity of the phosphors was observed with an increase in temperature, owing to the thermal quenching effect [18,19]. Thermal quenching is a type of non-radiative transition in which the excited Eu^{2+} ions release some of their energy to the surrounding host lattice via vibration. In this manner, the excited ions return to the ground state without the emission of electromagnetic radiation. The thermal quenching of $\text{Ba}_2\text{Si}_5\text{N}_8:\text{Eu}^{2+}$ is compared to $\text{Yag}:\text{Ce}^{3+}$ which is previous reported [20]. This result indicate that luminescence intensity of $\text{Yag}:\text{Ce}$ is about 80% at 120 °C. But $\text{Ba}_2\text{Si}_5\text{N}_8:\text{Eu}^{2+}$ phosphors show 84~89% intensity at 120 °C. It means that it is more thermally stable than $\text{Yag}:\text{Ce}$ phosphor (Ref. 20).

3.5. Quantum efficiency of phosphors

The QE of a phosphor is an important parameter to be considered for practical applications [21,22]. We measured QE at excitation wavelength of 395 nm because the high absorption and quantum efficiency of $\text{Ba}_2\text{Si}_5\text{N}_8:\text{Eu}^{2+}$ at the excitation wavelength of 395 nm indicate that it matches well with the emission wavelength of GaN base LED chips. Table 2 and Fig. 5 present the $\text{QE}(\eta)$ value of the $\text{Ba}_2\text{Si}_5\text{N}_8:\text{Eu}^{2+}$ phosphors, as calculated by using the

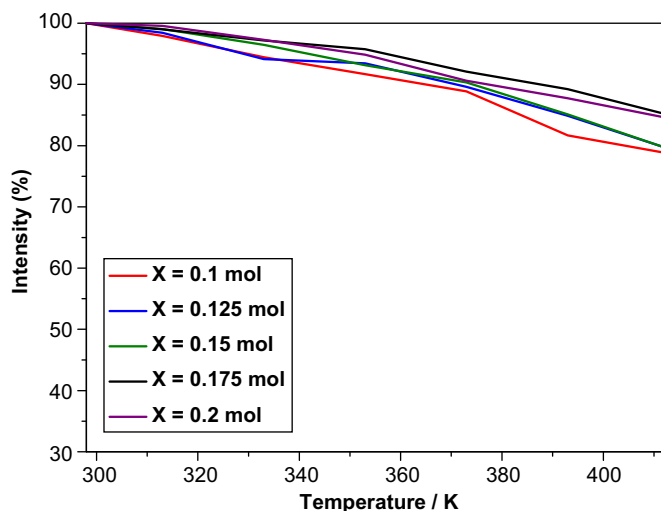


Fig. 4. Temperature dependence of PL intensity measured for $\text{Ba}_{2-x}\text{Si}_5\text{N}_8:\text{Eu}^{2+}$ upon excitation at 460 nm.

Table 2
Quantum efficiencies of Ba₂Si₅N₈ phosphors with different Eu²⁺ concentrations.

Eu ratio(mol)	Quantum efficiency at 395 nm
0.1	0.657
0.125	0.661
0.15	0.671
0.175	0.678
0.2	0.667

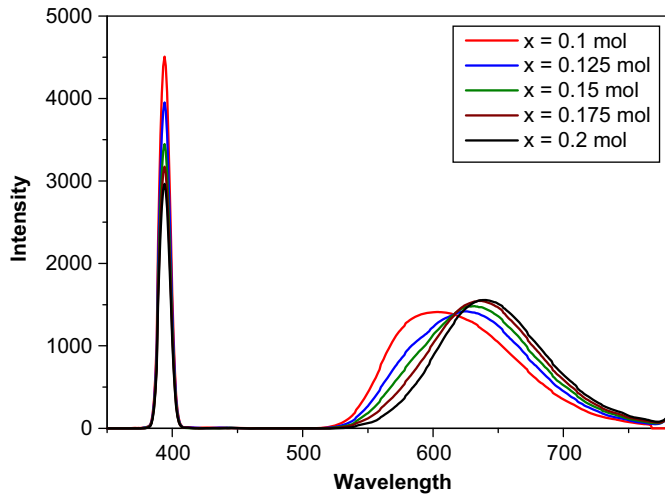


Fig. 5. Quantum efficiencies of Ba₂Si₅N₈ phosphors with different Eu²⁺ concentrations.

following equation [23].

$$\eta_{(\text{Internal})} = \frac{\int_{350}^{780} \lambda P(\lambda) d\lambda}{\int_{350}^{780} \lambda \{E(\lambda) - R(\lambda)\} d\lambda}$$

$$\eta_{(\text{External})} = \frac{\int \lambda P(\lambda) d\lambda}{\int \lambda E(\lambda) d\lambda}$$

where $E(\lambda)/h\nu$, $R(\lambda)/h\nu$, and $P(\lambda)/h\nu$ are the number of photons in the spectrum of excitation, reflectance, and emission of the phosphor, respectively. In this equation, where 350 nm and 780 nm are the shortest and longest wavelengths of interest, $E(\lambda)$ is the light energy reflected from reference, $R(\lambda)$ is the light energy reflected from the sample, and the $P(\lambda)$ is the PL light energy. We used sample holder which controls the thickness of powder sample, because the thickness of powder sample has to be considered as a factor affecting the absolute value of η . At 395 nm, the QE values of the Ba₂Si₅N₈:Eu²⁺ phosphors were 65.7%, 66.1%, 67.1%, 67.8%, and 66.7%, respectively. The data indicated that 0.175 mol Eu²⁺ doped Ba₂Si₅N₈:Eu²⁺ has the highest QE. The QE as well as PL intensity increased when the Eu²⁺ concentration x was increased to 0.175 mol and then decreased. These results showed the high efficiency of the concentrated

phosphor at $x=0.175$ mol and suggested that Eu²⁺ was an effective activator at this concentration.

4. Conclusions

Eu²⁺ activated red-emitting Ba₂Si₅N₈ phosphors were successfully produced using NPS by heating at 1620–1700 °C for 2 h under 70% N₂+30% H₂ flow. All the Ba₂Si₅N₈:Eu²⁺ compounds crystallized in an orthorhombic unit-cell(JCPDS 97-040-1501) but contained impurities attributed to some unknown secondary phase. The lattice size decreased with an increase in the concentration of Eu²⁺ decreased almost linearly with an increase in x , because of to the replacement of Ba²⁺ with the smaller Eu²⁺ ions, in keeping with Vegard's law. The emission peaks red-shifted from 593 nm to 633 nm when the Eu²⁺ concentration was varied from 0.1 mol to 0.2 mol at intervals of 0.025 mol. The fluorescence intensity increased with x and reached a maximum at $x \sim 0.175$ mol but decreased then on because of the concentration quenching effect. With an increase in temperature, the emission intensity of the phosphors reduced gradually owing to the temperature quenching effect. The average particle sizes of the Ba₂Si₅N₈:Eu²⁺ powders were about 1.12 ± 0.5 , 0.86 ± 0.2 , 1.42 ± 0.7 , 1.12 ± 0.5 , and 1.52 ± 0.4 μm , respectively. At 395 nm, the QE values of the Ba₂Si₅N₈:Eu²⁺ phosphors were 65.7%, 66.1%, 67.1%, 67.8%, and 66.7%, respectively. Thus, it could be concluded that Ba₂Si₅N₈:Eu²⁺ phosphors show outstanding luminescence efficiency at $x=0.175$ mol.

References

- [1] H. watanabe, N. Kijima, Crystal structure and luminescence properties of Sr_xCa_{1-x}SiN₃:Eu²⁺ mixed nitride phosphors, Journal of Alloys and Compounds 475 (2009) 434–439.
- [2] K. Uheda, N. Hiroaki, H. Yamamoto, Host lattice materials in the system Ca₃N₂-AlN-Si₃N₄ for white light emitting diode, Physica Status Solid(A) 203 (2006) 2712–2717.
- [3] Y.Q. Li, J.E.J. van Steen, A.C.A. Delsing, F.J. D Ivo, G. de, H.T. Hintzen, Luminescence properties of red-emitting M₂Si₅N₈:Eu²⁺ (M=Ca, Sr, Ba) LED conversion phosphors, Journal of Alloys and Compounds 417 (2006) 273–279.
- [4] X. Teng, W. Zhuang, Y. Hu, X. Huang, Luminescence properties of nitride red phosphors for LED, Journal of Rare Earths 26 (2008) 652–655.
- [5] R. Mueller-Mach, G. Mueller, M.R. Krames, H.A. Hoppe, F. Stadler, W. Schnick, T. Juestel, P. Schmidt, Highly efficient all-nitride phosphor-coverted white light emitting diode, Physica Status Solidi A 202 (2005) 1727–1732.
- [6] C.J. Duan, W.M. Otten, A.C.A. Delsing, H.T. Hintzen, Preparation and photoluminescence properties of Mn²⁺-activated M₂Si₅N₈ (M=Ca, Sr, Ba) phosphor, Journal of Solid State Chemistry 181 (2008) 751–757.
- [7] G. Blasse, Luminescent Materials, Berlin, Springer, 1994.
- [8] G. Blasse, Luminescence of rare earth ions at the end of the century, Journal of Alloys and Compounds 192 (1993) 17–21.
- [9] C.R. Ronda, Rare earth phosphors: fundamentals and application, Journal of Alloys and Compounds 275–277 (1998) 669–676.
- [10] Y.Q. Li, G. de With, H.T. Hintzen, Luminescence properties of Ce³⁺-activated alkaline earth silicon nitride M₂Si₅N₈ (M=Ca, Sr, Ba) materials, Journal of Luminescence 116 (2006) 107–116.
- [11] G. Blasse, Special cases of divalent lanthanide emission, European Journal Of Solid State And Inorganic Chemistry 33 (1996) 175–184.

- [12] R.J. Xie, N. Hirotsaki, Y. Li, T. Takeda, Rare-earth activated nitride phosphors: synthesis, luminescence and application, *Materials* 3 (2010) 3777–3793.
- [13] S. Ye, Z.S. Liu, X.T. Wang, J.G. Wang, L.X. Wang, X.P. Jing, Emission properties of Eu^{2+} , Mn^{2+} in $\text{MAl}_2\text{Si}_2\text{O}_8$ ($\text{M}=\text{Sr}$, Ba), *Journal of Luminescence* 129 (2009) 50–54.
- [14] Y. Umetsu, S. Okamoto, H. Yamamoto, Photoluminescence properties of $\text{Ba}_3\text{MgSi}_2\text{O}_8:\text{Eu}^{2+}$, Mn^{2+} (A and B=alkaline-earth metal) under near-UV pumped white LED application, *Journal of the Electrochemical Society* 155 (2008) J193–J197.
- [15] R.D. Shannon, Revised effective ionic radii and systematic studies of interatomic distances in halides and chalcogenides, *Acta Crystallographica A* 32 (1976) 751–767.
- [16] H.A. Hoppe, H. Lutz, P. Morys, W. Schnick, A. Seilmeier, Luminescence in Eu^{2+} -doped $\text{Ba}_2\text{Si}_5\text{N}_8$: fluorescence, thermoluminescence, and up-conversion, *Journal of Physics and Chemistry of Solids* 61 (2000) 2001–2006.
- [17] D.L. Dexter, A theory of sensitized luminescence in solid, *Journal of Chemical Physics* 21 (1953) 836.
- [18] V. Bachmann, C. Ronda, A. Meijerink, Temperature Quenching of Yellow Ce^{3+} Luminescence in $\text{YAG}:\text{Ce}$, *Chemistry of Materials* 21 (10) (2009) 2077.
- [19] P. Dorenbos, Thermal quenching of Eu^{2+} 5d-4f luminescence in inorganic compounds, *Journal of Physics: Condensed Matter* 17 (2005) 8103–8111.
- [20] P. Feofilov, D.V. Arsenyev, A.B. Kulinkin, T. Gacoin, G. Mialon, R.S. Meltzer, C. Dujardin, Gaseous environment-sensitive fluorescence of $\text{YAG}:\text{Ce}^{3+}$ nanocrystals, *Journal of Applied Physics* 107 (2010) 064308.
- [21] M. Zachau, Photocalorimetric measurement of the quantum efficiencies of phosphors, *Journal of Luminescence* 72–74 (1997) 792–793.
- [22] Y.Q. Li, G. de With, H.T. Hintzen, The effect of replacement of Sr by Ca on the structural and luminescence properties of the red-emitting $\text{Sr}_2\text{Si}_5\text{N}_8:\text{Eu}^{2+}$ LED conversion phosphor, *Journal of Solid State Chemistry* 181 (2008) 515–524.
- [23] K. Ohkubo, T. Shigeta, Absolute fluorescent quantum efficiency of NBS phosphor standard samples, *Journal of the Illuminating Engineering Institute of Japan* 83 (1999) 87–93 in Japanese.